

Micro-thermal focusing field-flow fractionation

Josef Janča^{a,*}, Irina A. Ananieva^{a,1}, Anastasija Yu. Menshikova^b, Tatiana G. Evseeva^b

^a *Pôle Sciences et Technologie, Université de La Rochelle, Avenue Michel Crépeau, 17042 La Rochelle Cedex 01, France*

^b *Institute of Macromolecular Compounds, Russian Academy of Sciences, 31 Bolshoi pr., 199004 St. Petersburg, Russia*

Abstract

Focusing mechanism was effectively exploited to separate large (micrometer-size) particles by using new micro-thermal field-flow fractionation (micro-TFFF). It has been shown that the retention order of micrometer-size particles at high field strength can be explained by the mechanism of steric exclusion only at lowest flow rates of the carrier liquid. A simplistic, purely mechanical model of steric exclusion is not accurate to describe the retention at higher flow rates where the focusing phenomenon appears. Despite the fact that the thickness of the channel for micro-FFF cannot be reduced without taking into account a possible deterioration of the separation due to the contribution of “steric exclusion” mechanism, this paper demonstrates, in agreement with our previous results, that if the operational conditions were conveniently chosen, namely a low flow rate, a reasonable fit of the experimental retention data with the theory of steric exclusion mechanism in FFF was found and the separation of micron-size particles can be accomplished. However, high selectivity and resolution and high-speed separation were achieved if the focusing effect has clearly dominated the FFF mechanism. As a result, it seems that the micro-TFFF is the most universal technique which can be applied for the separation of the synthetic and natural macromolecules within an extended range of molar masses up to ultra-high molar masses and for the particles of various chemical nature and origin in a nano-size range as well as for large (micrometers) particles. Until nowadays, only sedimentation and flow field-flow fractionation techniques in so called “steric” modes were applied for the separations of large size particles. This application of micro-TFFF in focusing mode for the separation of large size particles is the first one described in the literature.

© 2003 Elsevier B.V. All rights reserved.

Keywords: Micro-thermal field-flow fractionation

1. Introduction

The mechanism of separation in normal (polarization) field-flow fractionation (FFF) is based on the interaction of the retained species with the physical field acting across a thin channel, perpendicularly to the flow of a carrier liquid. Carrier liquid flowing along the channel forms a nearly parabolic flow velocity profile across the channel. Each retained species forms a nearly exponential concentration profile across the channel due to the field generated flux and the opposed diffusion flux. Larger species exhibiting lower diffusion coefficients are usually compressed closer to the accumulation wall in a zone of lower longitudinal velocity of the carrier liquid. The elution order is thus from the small to the large size species in this polarization mechanism. On the other hand, if the distances of the center of gravity of

the concentration profiles of the retained species from the accumulation wall are commensurable with their size, the elution order is inverted and the steric exclusion mechanism can govern the separation because the retained species cannot approach the accumulation wall closer than their radius and thus larger species elute with higher average longitudinal velocity. Such a situation appears if the field strength is high enough so that all species are compressed to the accumulation wall independently of their size. This mechanism has been exploited in steric mode FFF techniques. The first application was published by Giddings and Myers in 1978 [1], the other papers dealt exclusively with sedimentation/steric FFF or flow/steric FFF (see [2,3] for review).

Micro-thermal field-flow fractionation (micro-TFFF) is a new technique [4] that has already been applied to the separations of the macromolecules [4,5] and of the colloidal particles [6]. We have investigated recently [7] the effect of the steric exclusion mechanism on the retention of the fractionated species with regard to minimum thickness of the micro-TFFF channel that should be respected in order to avoid a deterioration of the separation of macro-

* Corresponding author. Tel.: +33-546458218; fax: +33-546421242.

E-mail address: jjanca@univ-lr.fr (J. Janča).

¹ Permanent address: Lomonosov Moscow State University, Lenin Hills, 119992 Moscow, Russia.

molecules and particles within as large molar mass and particle size ranges as reasonable. The results of the experiments carried out previously [7] with some colloidal and large size particles were used to prove the validity of our theoretical approach. On the other hand, the raised question was whether the experimental conditions can be chosen in such a manner that the steric exclusion mechanism would dominate the separation. In such a case, the micro-thermal/steric FFF could provide high performance and high-speed separations of the colloidal and large size (over 1 μm) particles.

Very spectacular experimental results of sedimentation/steric FFF were described by Koch and Giddings already in 1986 [8]. They separated polystyrene latex beads in the size range from 2 to 45 μm in the experiments carried out in FFF channel which was curved to fit within the rotor basket of a centrifuge. The separation of a mixture of seven different size beads was performed at high field strength and high flow rates in less than 4 min including the stop-flow period.

In 1982, Janča [9] proposed the application of the focusing mechanism in FFF resulting thus in a new method: focusing FFF. Giddings published in 1983 a paper [10] in which he proposed exactly the same separation mechanism but he preferred to call the technique “hyperlayer” FFF. The first detailed theory of focusing FFF was published in 1984 [11]. The theory was further developed in several publications, the references can be found in a summarizing paper on this topic [12]. Caldwell et al. [13] studied in 1984, a strong dependence of the retention ratio of human and animal cells on the flow rate and field strength, observed already earlier [14], and they explained this behavior by the lift forces emerging in sedimentation/“steric” FFF. Ratanathanawongs and Giddings [15] described in 1989 the active use of the focusing mechanism in flow FFF for high-speed characterization of silica particles with the conscious exploitation of the lift forces leading to the focusing phenomena.

In the mean time, several papers were published dealing with the investigation of the “steric”, “focusing”, or “hyperlayer” FFF mechanisms in which the lift forces played a role of a focusing force that must be position dependent according to the classical definition of the focusing mechanism (for example, in isopycnic or isoelectric focusing) adopted also in the theoretical approach concerning focusing FFF [12]. The corresponding references can be found in [2,3]. The focusing FFF principle can be used for the analytical separations of macromolecular and particular species but also for continuous preparative fractionation as proposed originally in 1984 [12] and used by Giddings in 1985 [16] under the term “split-flow lateral-transport thin” (SPLITT) separation cells for rapid and continuous particle fractionation. Regardless the terminological and historical cleavage, it became more and more evident that purely “steric” FFF represents rather an exceptional case of separation mechanism and that either various attractive forces between the

retained species and the accumulation wall in a close proximity of the wall or the opposing lift force (the magnitude of which increases with increasing flow velocity) frequently play a substantial role. Very often, the attractive forces between the retained species and the accumulation wall are so strong that some part of the sample is completely and irreversibly adsorbed on the wall. A well-known experimental observation that whenever the channel is opened for cleaning after an extensive use, a layer of the unidentified species can be seen on the accumulation wall thus confirming the important effect of the adsorption. Obviously, in such a case, the steric exclusion cannot well represent the accurate mechanism of FFF. On the other hand, whenever lift forces participate in FFF processes, the focusing mechanism is operating and, again, it is not steric exclusion mechanism that accurately describes the retention in FFF.

The important theoretical and experimental aspects concerning the questions how the concurrent increases in flow velocity and field strength should be chosen for optimum resolution and where are the ultimate limits of such a high-speed focusing (not steric) FFF strategy are not yet answered. This fact represents a challenge for micro-TFFF.

It has already been demonstrated in the above cited papers, that micro-TFFF seems to be the most universal of all FFF techniques driven by dominating polarization mechanism due to its capacity to separate the macromolecules within a large range of molar masses and the colloidal, sub-micron size particles. This study is aimed to show that even the separation of large size particles can effectively be performed by using micro-thermal/focusing FFF.

2. Theory

The retention ratio describing the simultaneous action of the normal (polarization) and steric exclusion mechanisms is [17]:

$$R = 6(\alpha - \alpha^2) + 6\lambda(1 - 2\alpha) \left[\coth \left(\frac{1 - 2\alpha}{2\lambda} \right) - \frac{2\lambda}{1 - 2\alpha} \right] \quad (1)$$

where $\alpha = r/w$ is the ratio of the radius r of the separated species to the thickness w of the separation channel and λ is a dimensionless retention parameter defined below. Whenever purely steric exclusion mechanism dominates the separation, the elution order is from the large to the small size species, while the elution order is usually inverted in dominating polarization mode FFF. For dominating steric exclusion mechanism the second term in Eq. (1) is equal to zero and thus we obtain:

$$R = 6\alpha(1 - \alpha) \quad (2)$$

For small α values, the Eq. (2) reduces to very simple relationship:

$$R = 6\alpha \quad (3)$$

Eqs. (1)–(3) are rigorously valid only if the flow velocity profile formed inside the channel is parabolic. This is not the case of micro-TFFF because the viscosity varies with the temperature across the channel and thus the flow velocity profile is not strictly parabolic and also the coefficient D_T (see below) is temperature dependent. Nevertheless, as can be seen in the following text, the use of the approximate Eqs. (1)–(3) is justified by the experimental results obtained by using micro-thermal focusing FFF.

When taking into consideration both polarization and steric FFF, limit value of R is given by [17]

$$\lim_{(\alpha, \lambda) \rightarrow 0} R = 6\gamma\alpha + 6\lambda \quad (4)$$

where γ is a dimensionless factor accounting for some non-idealities, for example for the frictional drag as proposed originally [17], but it can also account for the intervention of attractive or opposing lift forces. Correspondingly, γ can be higher or lower than one. The appearance of lift force in steric FFF was firstly described by Caldwell et al. [14], it was studied in more details by Williams et al. [18,19], but further extensive theoretical and experimental investigation of this aspect is certainly needed.

Retention parameter λ in Eq. (1), valid for hard spherical particles exhibiting the thermal diffusion, is given by [20]

$$\lambda = \frac{k_B T}{6\pi\eta r D_T \Delta T} \quad (5)$$

where k_B is Boltzmann constant, T is the temperature, η is the viscosity of the carrier liquid, D_T is the coefficient of thermal diffusion, and ΔT is temperature drop across the

micro-TFFF channel. By combining Eqs. (1) and (5), it is possible to obtain a convenient relationship describing the dependence of the retention ratio R on the diameter of the separated particles:

$$R = 6 \left(\frac{r}{w} - \left(\frac{r}{w} \right)^2 \right) + \frac{3sT}{r\Delta T} \left(1 - \frac{2r}{w} \right) \times \left[\coth \left(\frac{\Delta T(r - (2r^2/w))}{sT} \right) - \frac{sT}{\Delta T(r - (2r^2/w))} \right] \quad (6)$$

where s is defined by

$$s = \frac{2r\lambda\Delta T}{T} \quad (7)$$

The results of model calculations using the virtual operational parameters (corresponding to the real experimental conditions) are shown in Fig. 1 for three cases following from the original and truncated forms of Eq. (1) valid for limit situations when either α or λ approaches to zero. The lower monotonically decreasing curve in Fig. 1 corresponds to an idealized FFF case when exclusively polarization mechanism is operational. The apparent straight-line represents the retention ratio as a function of particle radius in the hypothetical case when exclusively steric exclusion mechanism is operational. At last, the upper curve exhibiting a minimum corresponds to the case when both mechanisms are effective but each one dominates the separation in its proper size range. The minimum corresponds to the inversion point as defined already by Giddings [17]. Obviously, the selectivity is low and the separation is deteriorated in the vicinity of the inversion point. The selectivity of separation by purely steric exclusion mechanism is lower in comparison with the selectivity when the polarization mechanism dominates, on the other hand, the band broadening in steric

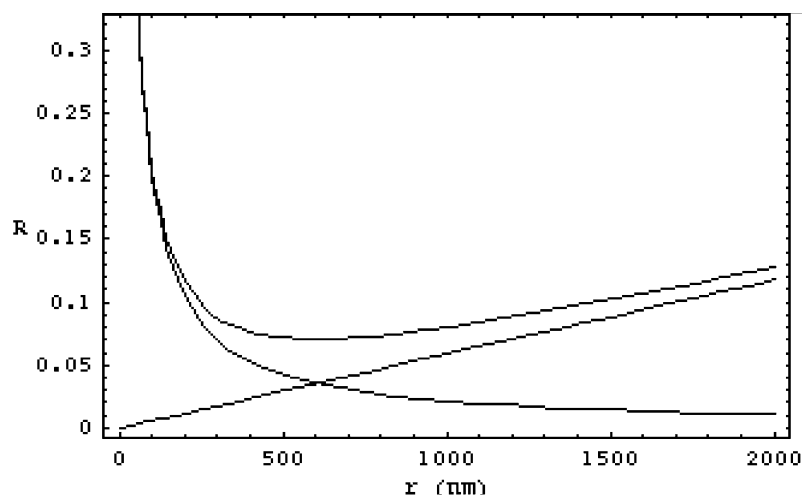


Fig. 1. Theoretical dependence of the retention ratio R on the particle radius r calculated from Eq. (6) by using $w = 0.01$ cm, $T = 293$ K, $\Delta T = 20$ K, and the slope, $s = 4.75 \times 10^{-8}$ cm, of the dependence $\lambda\Delta T/T$ vs. reciprocal value of the particle diameter $1/d_p$ (empirical value obtained previously [7]). Higher curve corresponds to original Eq. (6), lower curve corresponds to truncated Eq. (6) with $\alpha = 0$ (only polarization mechanism effective), and the apparent straight-line corresponds to truncated Eq. (6) with $\lambda = 0$ (only steric mechanism effective).

mode is substantially lower which makes the resolution attractive for high-speed separations.

3. Experimental

The apparatus for micro-TFFF consisted of a syringe pump model IPC 2050 (Linnet Compact, Czech Republic) or an intelligent pump model PU-980 (Jasco, Japan), an injection valve model 7410 (Rheodyne, USA) with a 1 μ l loop, a UV-Vis variable wavelength detector model UV-975 (Jasco, Japan) equipped with the 1 μ l cell, and an integrator Model HP 3395 (Hewlett-Packard, USA). The versatile micro-TFFF channel was designed in our laboratory and fabricated by Lascialfari, SARL (La Rochelle, France). The dimensions of the micro-channel used in this work were 0.1 mm \times 4 mm \times 96 mm. The cold wall temperature was controlled and kept constant by using a compact, low temperature thermostat Model RML 6B (Lauda, Germany). The electric power for heating cartridge was regulated by an electronic device designed and built up in our laboratory. The temperatures of the cold and hot walls were measured by digital thermometer (Hanna Instruments, Portugal) equipped with two thermocouples. An aqueous solution of 0.1% detergent Brij 78 (Fluka, Germany) and of 0.02% of NaCl was used as the carrier liquid.

Spherical carboxylated polystyrene latex particles (PS) were used in this study. Their synthesis was carried out in a four-necked glass reactor equipped with a glass paddle-type stirrer, condenser, nitrogen inlet and temperature controller. Continuous stirring at a rate of about 300 rpm was maintained during the polymerization process. All latex samples were prepared by polymerization of styrene using 4,4'-azo-bis-(4-cyanopentanoic) acid (CPA) as initiator (0.2 wt.%) at the temperature 353 ± 1 K. Table 1 lists the

Table 1
Composition and size characteristics of synthesized particles

Sample no.	Concentration of -COOH groups (μ g eq./m ²)	Particle diameter from TEM ^a (μ m)	Particle diameter from QELS (μ m)
PS1	0.4	0.100	0.118
PS2	1.8	0.250	0.302
PS3	2.2	0.360	0.427
PS4	2.4	0.530	0.607
PS5	2.6	0.630	0.747
PS6	2.3	0.720	0.781
PS7	1.9	0.870	1.025
PS8	2.4	1.000	1.045
PS9	2.3	1.140	1.523
PS10	1.6	1.360	1.891
PS11	2.9	1.430	1.387
PS12	2.5	1.900	1.961
PS13	2.8	2.300	2.300
PS14	4.2	2.500	2.473
PS15	2.5	3.200	3.211
PS16	2.7	3.800	3.769

^a Average particle diameters from TEM were used in all figures as values resulting in more coherent data series.

compositions of latex samples. Sample PS1 was synthesized in the presence of 6.1×10^{-3} mol/l sodium dodecyl sulfate (SDS) as an emulsifier, samples PS2 to PS8 were prepared by emulsifier-free polymerization technique [21–23]. In order to prepare PS particles of diameters over 1 μ m (samples PS9 to PS16), dispersion polymerization of styrene was carried out in the presence of poly(vinylpyrrolidone) (PVP) as a polymeric stabilizer in the ethanol/water mixture (93 vol.%) or in 100% ethanol [24]. After 4–7 h, a conversion of about 99% was reached. The latexes were washed by successive centrifugation and redispersion in water (at least three times). Finally, the samples were treated by ultrasound and kept in 10% water suspensions. The average particle sizes

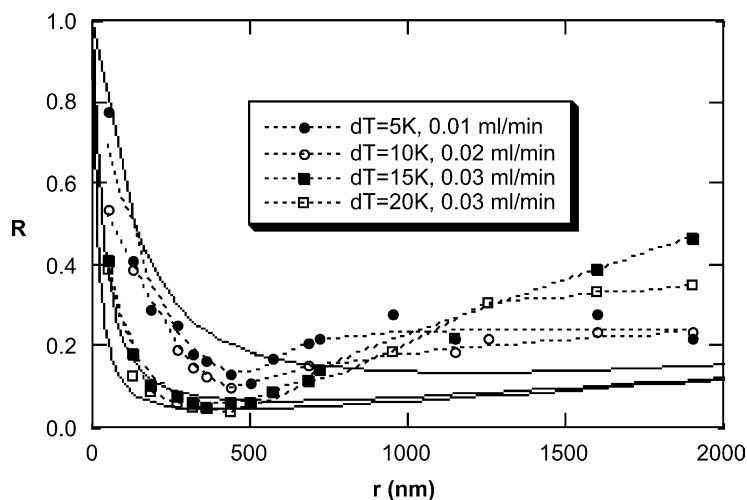


Fig. 2. Comparison of experimental retention data with the theoretical R vs. r curves calculated from Eq. (6) for $\Delta T = 5$ K (highest full curve), for $\Delta T = 10$ K (intermediate full curve), and for $\Delta T = 20$ K (lowest full curve), by using the same input data as in Fig. 1.

measured by quasi-elastic light scattering (QELS) and transmission electron microscopy (TEM) are given in Table 1.

The average particle diameters of all studied particles were measured by QELS by using Zetamaster (Malvern Instruments Ltd., Malvern, Worcestershire, UK) apparatus, and by TEM by using JEM 100 S microscope (Jeol, Japan). The analysis of micrographs of more than 100 particles of each sample gave their mean (by weight) diameter. The polydispersity index of all latex samples was lower than 1.02, indicating highly uniform particles. Surface concentration of carboxyl groups was determined by conductometric titration [25].

4. Results and discussion

The preliminary experiments were devoted to the measurement of the dependence of retention ratio on the particle radius within a large range of particle sizes from 100 to 3800 nm at different temperature drops $\Delta T = 5, 10, 15$ and 20 K and the flow rates varying from 0.01 to 0.03 ml/min. The results are shown in Fig. 2. The experimental points and the corresponding best-fit curves (dashed lines in Fig. 2) exhibit a good agreement with the theoretical (full-line) curves calculated for the appropriate experimental conditions in the range where normal, polarization mechanism dominates the

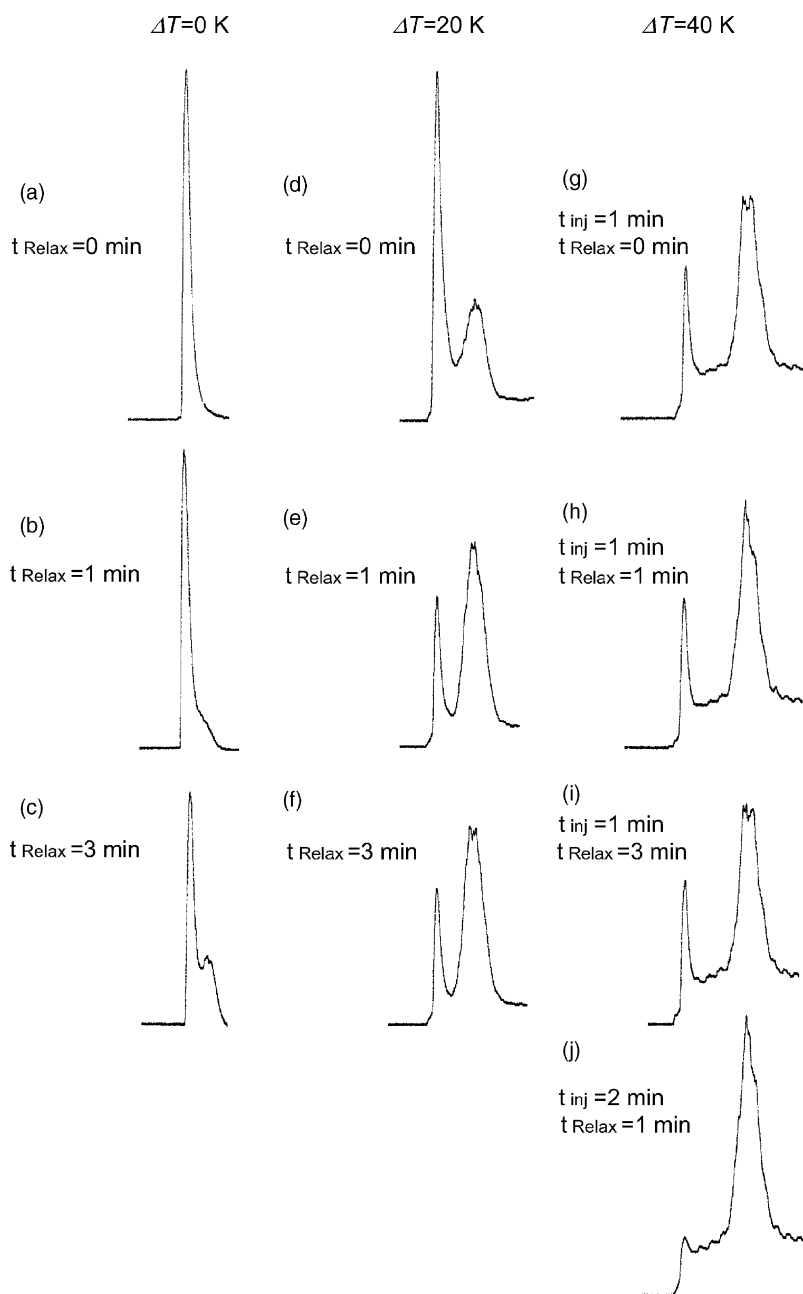


Fig. 3. Fractograms of the sample PS13 (2300 nm) obtained at various ΔT values and various relaxation (stop-flow) times. The flow rate during the injection was always 0.01 ml/min, the flow rate applied after the relaxation period was always 0.5 ml/min.

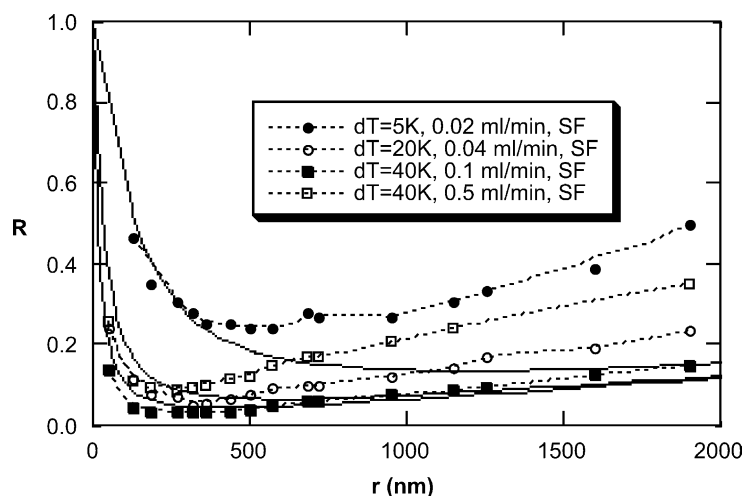


Fig. 4. Comparison of experimental retention data with the theoretical R vs. r curves calculated from Eq. (6) for $\Delta T = 5$ K (highest full curve), for $\Delta T = 10$ K (intermediate full curve), and for $\Delta T = 20$ K (lowest full curve), by using the same input data as in Fig. 1. The relaxation (stop-flow time) applied were 3 min at $\Delta T = 5$ K and $\Delta T = 20$ K, and 1 min at $\Delta T = 40$ K.

separation. On the other hand, in the range where the “steric exclusion” mechanism should (hypothetically) be operating, the experimental data deviate from the theoretical curves in an important manner. Although these preliminary experiments do not represent a systematic study, it is obvious that the deviations increase with increasing flow rate and with decreasing temperature drop. It has to be stressed that all experiments the results of which are shown in Fig. 2 were carried out without stopping the flow of the carrier liquid after the injection in order to reach a steady-state concentration distribution across the channel of the retained species from the very beginning of the FFF run.

Fig. 3 shows the effect of the mode of injection and of the relaxation time on the fractograms of a large size sample (diameter 2300 nm) obtained at relatively high flow rate applied after a relaxation period at different temperature drops.

The injection of the sample was always carried out at very low flow rate 0.01 ml/min during 1 min that was the time necessary to allow one that the whole sample volume is introduced into the channel. The fractograms *a*, *b*, and *c* show that the particles of this size sediment under the effect of the gravitational force and are weakly retained even if temperature drop was $\Delta T = 0$ K under the condition that enough relaxation time was applied at the beginning of the run. The fractograms *d*, *e*, and *f* show that the retention of the sample substantially increased with $\Delta T = 20$ K and that the relaxation time (stop-flow period) longer than 1 min has no more effect on the amount of the unrelaxed part of the sample. Further increase of temperature drop to $\Delta T = 40$ K resulted in an increase of the retention. The relaxation after the injection was so rapid that there is not difference between the fractograms *g*, *h*, and *i* obtained without stop-flow period or

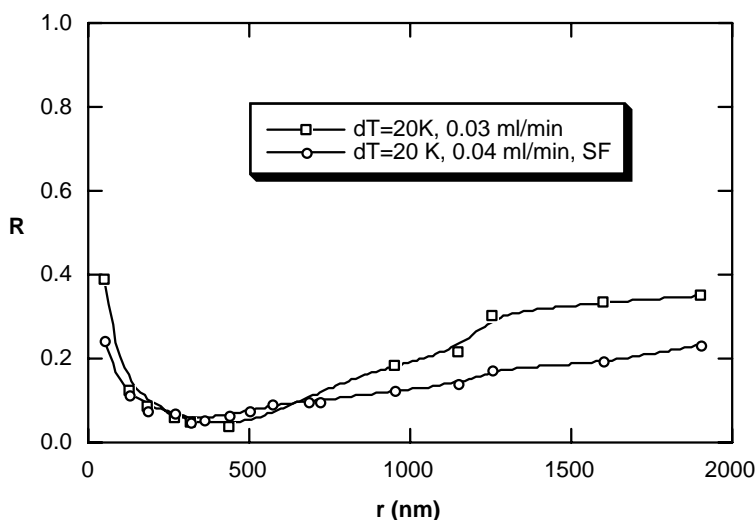


Fig. 5. Comparison of experimental retention data obtained under similar experimental conditions without and with the application of stop-flow time for relaxation.

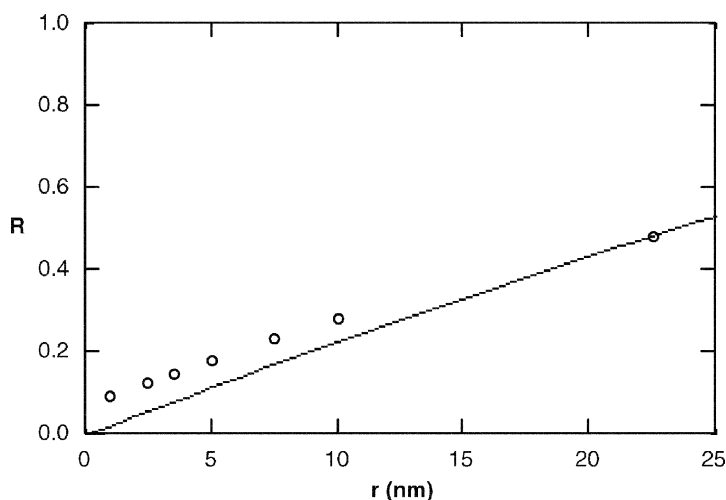


Fig. 6. Comparison of experimental retention data with the theoretical R vs. r curve calculated from Eq. (3). The experimental data were obtained from the fractogram in Fig. 5 shown in Ref. [8].

with different stop-flow times applied. On the other hand, a longer injection period at low flow rate resulted in more complete introduction of the sample into the channel and the relaxation peak practically disappeared (see fractogram *j*).

In the following experiments (see Fig. 4), the optimized injection-stop-flow procedures were applied. The injection at low flow-rate 0.01 ml/min was carried out during 1 min followed by stop-flow time 3 min at $\Delta T = 5$ K and $\Delta T = 20$ K and by stop-flow time 1 min at $\Delta T = 40$ K. The effect of the temperature drop and of the flow rate on the deviation of the experimental retentions from the theoretical dependences calculated for hypothetical dominating steric exclusion mechanism was confirmed also for these experiments performed with the application of a specific injection-stop-flow procedure. The only experiment carried out at $\Delta T = 40$ K and at low flow rate 0.1 ml/min exhibited a closest agreement with the theoretical retention curve corresponding to pure steric exclusion mechanism. Further decrease of the flow rate, nevertheless, resulted in only partial recovery of most of the samples going up to complete and irreversible retention, which means that short-range attractive interactions of the particles with the accumulation wall became effective. It could not, however, be confirmed that even in a narrow “window” of experimental conditions ($\Delta T = 40$ K and flow rate 0.1 ml/min) the mechanism of separation corresponds to steric exclusion and not to focusing.

In Fig. 5, we reproduced some above shown experiments carried out at almost identical experimental conditions with and without the application of optimized injection-stop-flow procedure just to stress the importance of such a procedure to obtain the accurate retention data corresponding to dominating focusing mechanism.

Although above described results represent the first demonstration of focusing TFFF with an active exploitation of lift forces, this mechanism is obviously not inherent

to micro-TFFF. Fig. 6 shows the experimental retentions calculated from the fractograms published by Koch and Giddings [8] in comparison with the theoretical dependence calculated for pure steric exclusion mechanism. The experimental points are well above the theoretical curve thus confirming the action of the focusing and not of the steric exclusion mechanism. Obviously, similar results could be obtained by comparing other published results with the theory. As a result, it seems to be the time to call the observed phenomena by more appropriate terminology in order to avoid the existing confusions and to respect the chronological priorities.

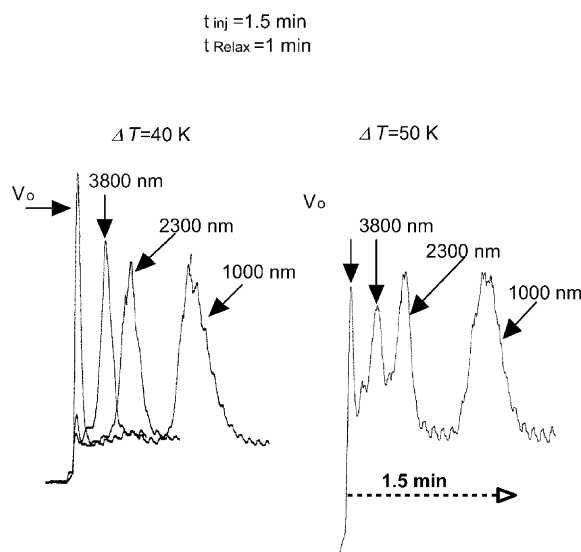


Fig. 7. Fractograms of the samples PS8, PS13, and PS16 obtained individually and in a mixture at $\Delta T = 40$ and 50 K, respectively, with the application of relaxation (stop-flow) times. The flow rate during the injections was 0.01 ml/min, the flow rate applied after the relaxation period was 0.5 ml/min.

5. Conclusion

Our investigation of micro-thermal focusing FFF will continue with the goal to develop further this high-speed and high-performance method of separation and characterization of large size particles. The first results are demonstrated in Fig. 7 which shows a superposition of the fractograms of individually injected samples of different size particles under the optimized experimental conditions. This result was very promising and a real separation of a mixture of the concerned samples shown also in Fig. 7 confirmed that it is possible to achieve such a high-speed high-performance separation by micro-thermal focusing FFF.

Acknowledgements

This work was supported by Regional Council of Poitou-Charentes and by Russian Foundation for Basic Research (project no. 01-03-32414) and by Program of Division of Chemistry and Material Sciences of Russian Academy of Sciences.

References

- [1] J.C. Giddings, M.N. Myers, *Sep. Sci. Technol.* 13 (1978) 637.
- [2] J. Janča, *Field-Flow Fractionation: Analysis of Macromolecules and Particles*, Marcel Dekker, New York, 1988.
- [3] M.E. Schimpf, K.D. Caldwell, J.C. Giddings, *Field-Flow Fractionation Handbook*, Wiley, New York, 2000.
- [4] J. Janča, *J. Liq. Chromatogr. Rel. Technol.* 25 (2002) 683.
- [5] J. Janča, *J. Liq. Chromatogr. Rel. Technol.* 25 (2002) 2173.
- [6] J. Janča, *Collect. Czech. Chem. Commun.* 67 (2002) 1596.
- [7] J. Janča, I.A. Ananieva, *e-Polymer* (34) (2003).
- [8] T. Koch, J.C. Giddings, *Anal. Chem.* 58 (1986) 994.
- [9] J. Janča, *Makromol. Chem., Rapid. Commun.* 3 (1982) 887.
- [10] J.C. Giddings, *Sep. Sci. Technol.* 18 (1983) 765.
- [11] J. Janča, J. Chmelik, *Anal. Chem.* 56 (1984) 2481.
- [12] J. Janča, *Collect. Czech. Chem. Commun.* 66 (2001) 1191.
- [13] K.D. Caldwell, Z.-Q. Cheng, P. Hradecky, J.C. Giddings, *Cell Biophys.* 6 (1984) 233.
- [14] K.D. Caldwell, T.T. Nguyen, M.N. Myers, J.C. Giddings, *Sep. Sci. Technol.* 14 (1979) 935.
- [15] S.K. Ratanathanawongs, J.C. Giddings, *J. Chromatogr.* 467 (1989) 341.
- [16] J.C. Giddings, *Sep. Sci. Technol.* 20 (1985) 749.
- [17] J.C. Giddings, *Sep. Sci. Technol.* 13 (1978) 241.
- [18] S.P. Williams, T. Koch, J.C. Giddings, *Chem. Eng. Commun.* 111 (1992) 121.
- [19] S.P. Williams, M.H. Moon, Y. Xu, J.C. Giddings, *Chem. Eng. Sci.* 51 (1996) 4477.
- [20] J. Janča, *J. Liq. Chromatogr. Rel. Technol.* 26 (2003) 835.
- [21] L.S. Lishanskii, A.Yu. Menshikova, T.G. Evseeva, et al., *Vysokomol. Soedin.* 33 (1991) 413.
- [22] A.Yu. Menshikova, T.G. Evseeva, B.M. Shabsels, et al., *Kolloidn. Zh.* 59 (1997) 620.
- [23] V. Shubin, Yu. Samoshina, A.Yu. Menshikova, T.G. Evseeva, *Colloid Polym. Sci.* 275 (1997) 655.
- [24] B. Thompson, A. Rudin, G. Lajoie, *J. Polym. Sci., Part A* 33 (1995) 3.
- [25] V.T. Labib, A.A. Robertson, *J. Colloid Interface. Sci.* 17 (1980) 151.